CHINESE OPTICS LETTERS
Vol. xx, No. x | February 2024

Observation of optical rogue waves in 2D optical lattice

Meng Li (李 萌), Jie Song (宋 洁), Fuqiang Li (李富强), Cibo Lou (楼慈波)*
School of Physical Science and Technology, Ningbo University, Ningbo 315211, China

***Corresponding author:** loucibo@nbu.edu.cn
Received Month X, XXXX | Accepted Month X, XXXX | Posted Online Month X, XXXX

We use a broad Gaussian beam with perturbations to motivate rogue waves in a two-dimensional optical induced lattice. In a linear situation, we fail to observe RWs. Nevertheless, under a nonlinear condition, the probability of RWs in the lattice is less than that in a homogeneous medium. Additionally, we obtain a shorter long-tails distribution of probability density function in an optical lattice.

Keywords: optical rogue waves, spatial rogue waves, optical induced lattice.
DOI: xxxxxxx/COLxxxxxxx.

1. Introduction

In 2007, Solli observed optical rogue waves (RWs) during the investigation of supercontinuum in optical fibers [1] . Optical RWs were statistically associated with long-tails distributions. It has been studied in several optical systems, such as fibers [2–4], optical waveguides [5,6], and gratings [7–9]. Generally, RWs are generated by a nonlinear process known as modulation instability (MI) [10–13], which is a complex process and highly sensitive to initial conditions. However, most previous researches focus on temporal RWs, with considerably less emphasis on spatial RWs. Research on spatial RWs is increasing in recent years. In biased strontium barium niobate (SBN) crystals, RWs were induced by a narrow Gaussian beam [14]. They discovered that the probability of RWs occurrence increased with the applied electric field. Chen found that a broad Gaussian beam with perturbations also generated RWs in biased SBN crystals [15]. But the probability distribution of RWs displayed a breathing behavior. Most RWs are generated by MI, which has been also studied in periodic structures. In pyroelectric crystals [16], the increase rates of MI was influenced by the external biased field. In magnonic crystals [17], MI was observed only at the frequencies corresponding to the band gaps of the crystal. Optical lattices enable precise control and adjustment of the light field, establishing them as crucial tools for the investigation of optical phenomena. Gomila reported that the band gap in an optical lattice may hinder the occurrence of MI [18]. Li demonstrated that a plane wave with perturbations could generate PS solitons with RWs waveforms in the periodic potential [19]. Rivas reported on the first experiments of rogue waves in 1D disordered photonic lattices [20]. However, the experiments and statistical results of extreme events in 2D optical lattice were not investigated yet.

In this paper, we conduct experimental investigations on high-amplitude events within a two-dimensional optical induced lattice [21] in biased SBN crystal. Our experiment is carried out by injecting a noise-seeded broad Gaussian into the lattice. Through the analysis of optical patterns on the output plane of SBN, we examine the transport of the probe beam under both linear and nonlinear conditions. Furthermore, we calculate the probability of RWs and compare it with that in a homogeneous medium.

2. Experiment

The experimental setup is shown in Fig. 1(a). The wavelength of laser beam is 532 nm. It is split into two beams by BS1. One beam is employed as the 2D lattice induced light. Power of induced light is 530 μW and it is ordinarily-polarized. A 2D optical diamond lattice [shown in Fig. 1(c)] with a period of 23 μm is established by sending the induced light through a mask. The lattice remains nearly invariant as it traverses the SBN crystal with cross-sectional dimensions of 5 mm × 5 mm and a length of 10 mm. In addition, the spatial spectrum of the lattice is obtained using the spectrum imaging subsystems demonstrated in Fig. 1(a). When the biased voltage U < 800 V, the first photonic band does not open. As shown in Fig. 1(d), the periodic structure's first photonic band gap is opened with U = 800 V. When U > 800V, the diffusion effect in SBN is raised, resulting in increased complexity of the nonlinear processes within the system. A broad Gaussian beam, split from the same laser but extraordinarily-polarized, is used as the probe beam. The

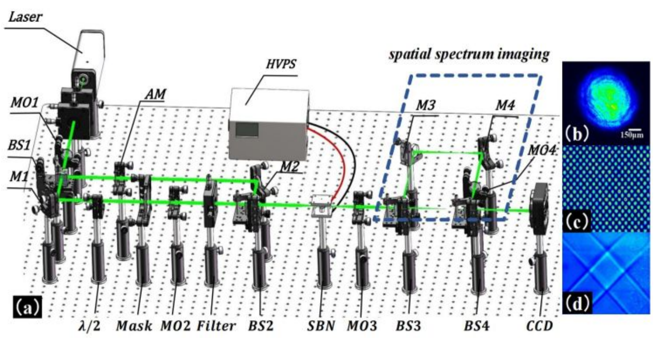

Fig. 1. (a)Experimental setup for observing RWs, the blue square is used to observe the spectrum of lattice. BS: Beam spliter. AM: Amplitude mask. HVPS: High-voltage power supply. (b)Probe light at the front plate of SBN. (c)The induced lattice beams in SBN crystal. (d)The Brillouin zone of the lattice.

beam width is approximately 450 μm, as shown in Fig. 1(b). Perturbations applied to it are provided by the amplitude mask(AM). Probe beam is injected into the crystal and propagates collinearly with the lattice. The adjustment of nonlinearity is controlled by the biased voltage. Optical patterns at the output plane of SBN are recorded by the CCD camera.

As the probe beam propagates in the optical lattice, monitoring of linear and nonlinear transport is obtained by recording its instantaneous and steady-state output patterns from the lattice. Fig. 2 (a) and Fig. 2 (b) demonstrate typical output patterns observed in linear and nonlinear situations (U = 800 V), respectively. In Fig. 2(b), several light waves with significantly high amplitude are visible.

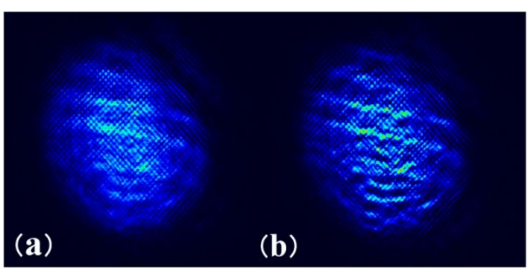

Fig. 2. In the experiment, the output patterns of the probe beam in the lattice in (a) linear and (b) nonlinear situations. U = 800 V.

According to the definition of space rogue waves [22], light beams exceeding twice the effective intensity (I_e) can be classified as extreme events (EEs). The I_e is defined as the average of the first third of the waves with the highest intensity. Events with an abnormality index (AI = I/I_e > 2) are considered as RWs [23]. The experiment was repeated 30 times under different initial conditions, and over 7000 waves were used for statistical analysis. A total of 225 waves were identified as RWs. Additionally, we replicated the aforementioned experiment in a homogeneous medium. The probability density function (PDF) of AI in different media is shown in Fig. 3. A gray dashed line at AI = 2 is a criterion to determine RWs. In the nonlinear situation, probability of RWs in the homogeneous medium is about 13%. The PDF curve(red triangles) with long tails is similar to that of Nakagami-m distribution(m<0.25). In this case, extremely high peak beams are generated. The maximum value of AI is 7.9. Nevertheless, probability of RWs decreases from 13% in the homogeneous medium to 8% in the optical lattice. There is a significant shortening of the long-tails in the lattice (blue circles) compared to a homogeneous medium (red triangles). And the maximum value of AI is 3.9. Under linear condition, no beams exceeding the gray dashed line were observed. We fail to observe RWs (black square).

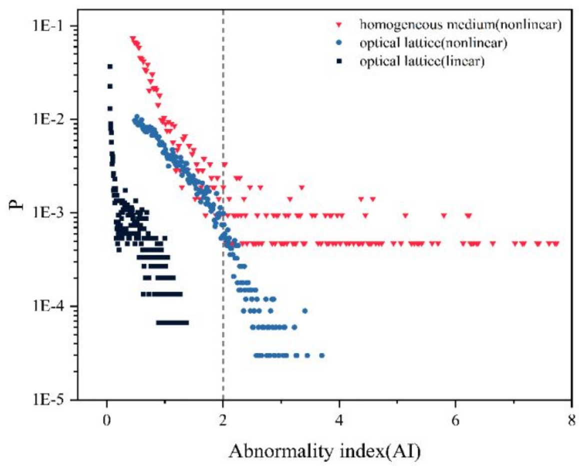

Fig. 3. The experimental results of the PDF for AI in an optical lattice (blue circle) and in a homogeneous medium (red triangles) under a nonlinear condition, in an optical lattice under a linear condition (black square). U = 800 V.

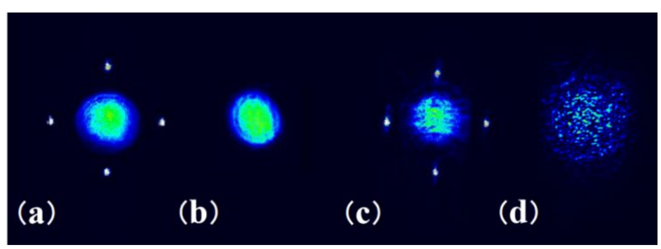

Fig. 4. The spectra of the probe beam in (a) (c) an optical lattice and (b) (d) a homogeneous medium under linear and nonlinear conditions, respectively. U = 800 V.

The phenomenon is primarily attributed to the lattice structure. In a linear situation, the probe beam propagates evenly through an array of waveguides(see Fig. 4(a)). We failed to observe RWs under these conditions(shown in Fig. 3(black square)). However, under the nonlinear condition, the MI generated from perturbations in the probe beam is hindered by the band gap of the lattice. Consequently, the probe beam is limited to only propagating in the first band(Fig. 4 (c)). Under nonlinear effects, RWS is generated within the lattice(shown in Fig. 3(blue circle)). In contrast, a homogeneous medium does not posses such restrictions, as displayed in Fig. 4 (d). We can observe RWs in this conditions(shown in Fig. 3(red triangles)). In optical lattice, filamentary collisions are not as common as in a homogeneous medium due to lattice waveguides limitations. As a result, the probability of RWs in the lattice decreases significantly.

3. Numerical Simulation

The distributed beam propagation method [24] is used in numerical simulations to verify the results generated experimentally. The dimensionless nonlinear Schrödinger equation used in the simulation is as follows:

$$i\frac{\partial\psi(x,y,z)}{\partial z}+\beta\nabla_{\perp}^{2}\psi(x,y,z)+\alpha\psi(x,y,z)=0. \qquad (1)$$

In this formula, z represents the propagation distance, ψ denotes the slowly varying light wave envelope, and β signifies the diffraction coefficient. The Laplacian operator is denoted as $\nabla_{\perp}^{2}$. In Eq. 1, the nonlinear coefficient α is

$$\alpha=\left(\frac{\kappa}{1+|\psi(x,y,z)|^{2}}+\Delta\eta\right). \qquad (2)$$

First part of Eq. 2 used to describe the saturation nonlinearity. The nonlinearity is regulated through the adjustment of κ. Periodic refractive index modulations are provided by $\Delta\eta$. A broad Gaussian beam with 20% perturbation is employed as the probe light. Similar to the experiment, the nonlinear propagation of light waves in periodic and homogeneous media is investigated in our simulations. Fig. 5 illustrates the cross-section of

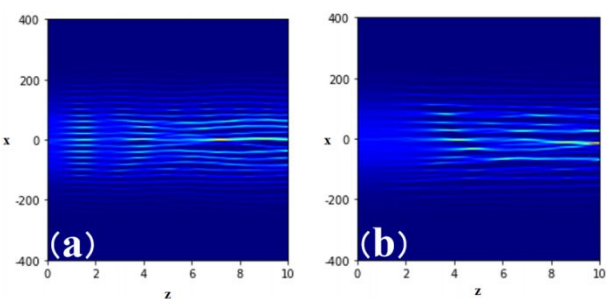

Fig. 5. The propagation of probe beam in (a) an optical lattice and (b) a homogeneous medium in numerical. κ = 2.

propagation at κ =2.

In comparison to a homogeneous medium, light is limited by an array of waveguides while propagating in a lattice, as illustrated in Fig. 5(a). Moreover, there is a significant decline in wave-to-wave collisions in the homogeneous medium, as depicted in Fig. 5(b). The simulation is repeated 1000 times under different initial conditions, and Fig. 6 presents the PDF of AI in two different media.

Fig. 6 is corresponding to the Fig. 3. The trend of the curves in both figures is roughly the same. In homogeneous medium, the probability of RWs is 15.8%(red triangles). And the maximum value of AI is 7.7. Furthermore, the probability of the RWs in the optical lattice is 6.5%(blue circle). It is also less than that in the homogeneous medium. A shorter long-tails in the lattice is displayed. Under linear condition(black square), RWs cannot be observed numerically.

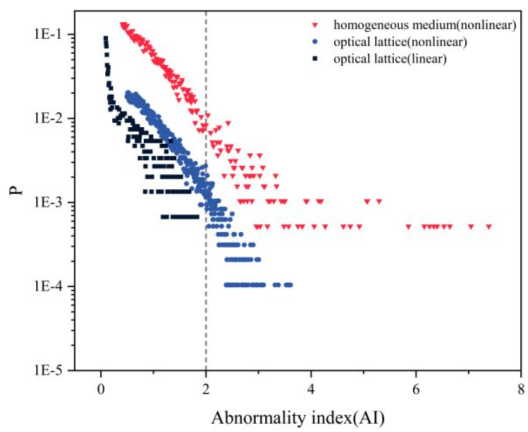

Fig. 6. The PDF of AI in optical lattice (blue circle), in homogeneous medium (red triangles) under nonlinear condition, and in optical lattice under linear condition (black square) numerically. κ = 2.

4. Conclusion

In summary, RWs are excited by a broad Gaussian light with perturbations in an 2D optical induced lattice. Due to the localization and band structure of the lattice, we can't observe RWs in linear situation. Conversely, under nonlinear condition, we observe a less probability of RWs and a shorter long-tails in an optical lattice compared to that in a homogeneous medium.

5. Acknowledgment

This research was funded by National Natural Science Foundation of China (No. 12074207).

References

1. D. R. Solli, C. Ropers, P. Koonath, and B. Jalali,"Optical rogue waves", Nature **450**, 1054 (2007).

2. D. Buccoliero, H. Steffensen, H. Ebendorff-Heidepriem, T. Monro, M. Tanya and O. Bang,“Midinfrared optical rogue waves in soft glass photonic crystal fiber”, Opt. Express **19**, 17973 (2011).
3. Q. Wang, X. Li, “Collision properties of rogue waves in optical fiber”,Opt. Commun. **435**, 255 (2019).
4. K. Hammani, B. Kibler, J. Fatome, S. Boscolo, G. Genty, J. M. Dudley, G. Millot, and C. Finot, “Nonlinear spectral shaping and optical rogue events in fiber-based systems”,Opt. Fiber Technol. **18**, 248 (2012).
5. R. Gupta, C. N. Kumar, V. M. Vyas, and P. K. Panigrahi, “Manipulating rogue wave triplet in optical waveguides through tapering”, Phys. Lett. A **379**, 314 (2015).
6. C. D. Pelwan, A. Quandt, and R. Warmbier, “Onset times of long-lived rogue waves in an optical waveguide array”, JOSA A **37**, C67 (2020).
7. A. Degasperis, S. Wabnitz, and A. B. Aceves, “Bragg grating rogue wave”, Phys. Lett. A **379**, 1067 (2015).
8. H. Kaur, Nisha, A. Goyal, T. S. Raju, and C. N. Kumar, “Generation and controlling of ultrashort self-similar solitons and rogue waves in inhomogeneous optical waveguide”, Optik **223**, 165634 (2020).
9. S. K. Gupta and A. K. Sarma, “Periodic optical rogue waves (PORWs) in parity-time (PT) symmetric Bragg-grating structure”, Europhys. Lett. **1620**, 452 (2014).
10. M. Onorato, S. Residori, U. Bortolozzo, A. Montina, and F. T. Arecchi, “Rogue waves and their generating mechanisms in different physical contexts”, Phys. Reports **528**, 47 (2013).
11. N. N. Akhmediev and V. I. Korneev, “Modulation instability and periodic solutions of the nonlinear Schr dinger equation”, Theor. Math. Phys. **69**, 1089 (1986).
12. G. Genty, J. M. Dudley, and B. J. Eggleton, “Modulation control and spectral shaping of optical fiber supercontinuum generation in the picosecond regime”, Appl. Phys. B **94**, 187 (2009).
13. J. M. Dudley, G. Genty, F. Dias, B. Kibler, and N. Akhmediev, “Modulation instability, Akhmediev breathers and continuous wave supercontinuum generation”, Opt. Express **17**, 21497 (2009).
14. C. Hermann-Avigliano, I. A. Salinas, D. A. Rivas, B. Real, A. Mančić, C. Mejía-Cortés, A. Maluckov, and R. A. Vicencio, “Spatial rogue waves in photorefractive SBN crystals”, Opt. Lett. **44**, 2807 (2019).
15. Z. Chen, F. Li, and C. Lou, “Statistical study on rogue waves in Gaussian light field in saturated nonlinear media”, Chin. Opt. Lett. **20**, 081901 (2022).
16. A. Katti and R. A. Yadav, “Modulation instability of broad optical beams in unbiased photorefractive pyroelectric crystals”, Chaos, Solitons Fractals **101**, 20 (2017).
17. A. V. Drozdovskii, B. A. Kalinikos, A. B. Ustinov, and A. Stashkevich, “Spin-wave self-modulation instability in a perpendicularly magnetized magnonic crystal”, J. Phys.: Conf. Ser. **769**, 012071 (2016).
18. D. Gomila, R. Zambrini, and G.-L. Oppo, “Photonic band-gap inhibition of modulational instabilities”, Phys. Rev. Lett. **92**, 253904 (2004).
19. S. Li, Y. Cheng, and F. Chang, “Generation and Modulation of Rogue Waves on Periodic Background”, Acta Photonica Sin. **49**, 619001 (2020).
20. D. Rivas, A. Szameit, and R. A. Vicencio, “Rogue waves in disordered 1D photonic lattices”, Sci. Rep.**10**, 13064 (2020).
21. N. Zhu, Z. Liu, R. Guo, and S.-M. Liu, “A method of easy fabrication of 2D light-induced nonlinear photonic lattices in self-defocusing LiNbO3:Fe crystal”, Opt. Mater. **30**, 527 (2007).
22. J. He, S. Xu, and K. Porsezian, “N -order bright and dark rogue waves in a resonant erbium-doped fiber system”, Phys. Rev. E **86**, 066603 (2012).
23. M. G. Clerc, G. González-Cortés, and M. Wilson, “Extreme events induced by spatiotemporal chaos in experimental optical patterns”, Opt. Lett. **41**, 2711 (2016).
24. F. Chen, M. Stepić, C. E. Rüter, D. Runde, D. Kip, V. Shandarov, O. Manela, and M. Segev, “Discrete diffraction and spatial gap solitons in photovoltaic LiNbO3 waveguide arrays”, Opt. Express **13**, 4314 (2005).